01 Jan 2023

3D-Printed Boron Nitride Catalytic Monoliths For Oxidative Dehydrogenation Of Propane

Theodore Agbi

Wei Shang Lo

Khaled Baamran

Taekyung Ryu

et. al. For a complete list of authors, see https://scholarsmine.mst.edu/che_bioeng_facwork/1418

Recommended Citation

T. Agbi et al., "3D-Printed Boron Nitride Catalytic Monoliths For Oxidative Dehydrogenation Of Propane," *Topics in Catalysis*, Springer, Jan 2023.
The definitive version is available at https://doi.org/10.1007/s11244-023-01819-2

Topics in Catalysis
https://doi.org/10.1007/s11244-023-01819-2

ORIGINAL PAPER

3D-Printed Boron Nitride Catalytic Monoliths for Oxidative Dehydrogenation of Propane

Theodore Agbi[1] · Wei-Shang Lo[2] · Khaled Baamran[4] · Taekyung Ryu[2] · Christine Cheung[2] · Fateme Rezaei[4] · Ive Hermans[1,2,3]

Accepted: 19 April 2023

Abstract

Boron-containing materials are efficient catalysts for the oxidative dehydrogenation of propane to propylene, proceeding *via* radical intermediates. The radical mechanism is initiated by the solid surface and propagated in the gas phase. It has been hypothesized that the propylene selectivity could be increased by enhancing the gas-phase contributions by favoring the formation of *iso*- over *n*-propyl radical intermediates. Indeed, whereas *n*-propyl radicals can be converted to both propylene and ethylene, *iso*-propyl radicals yield exclusively propylene. In this contribution, we explore 3D printing to structure the hexagonal boron nitride (hBN) heterogeneous catalyst with high void space. 3D-printed hBN monoliths were found to exhibit a higher olefin selectivity and a higher $r_{propylene}/r_{ethylene}$ ratio as compared to traditional pack beds of hBN pellets. Our kinetic studies indicate the increase of reaction order in propane from 1.5 to 2.3, implying the promotion of gas-phase reaction. This work does not only shows that 3D-structured catalysts lead to higher propylene selectivity, it also confirms the hypothesized reaction mechanism and illustrates the power of molecular insights in selective oxidation chemistry to improve the performance.

Graphical abstract

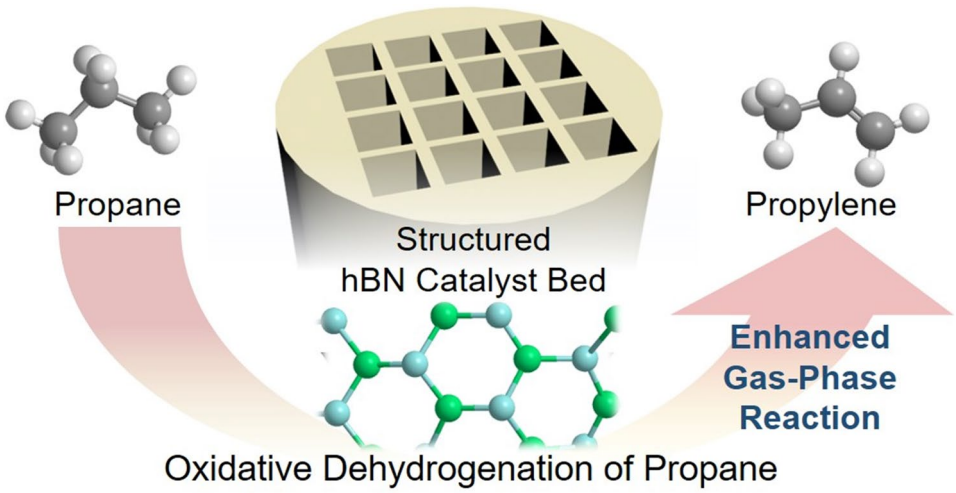

Keywords Boron-containing catalysts · Olefins · Oxidative dehydrogenation · Structured catalyst · 3D printing

✉ Fateme Rezaei
rezaeif@mst.edu

✉ Ive Hermans
hermans@chem.wisc.edu

Extended author information available on the last page of the article

Published online: 05 May 2023

1 Introduction

Hexagonal boron nitride and boron-containing materials recently emerged as promising catalysts for the oxidative dehydrogenation (ODH) of small alkanes, resulting in high olefin selectivity and minimal CO_x formation [1–3]. In 2016, our group showed that hBN afforded selectivity to propylene at 79% at a propane conversion of 14% [4], and the major byproduct observed in this reaction is ethylene (12%), rather than the carbon oxides (CO_x; combined selectivity of less than 4%) commonly observed with metal oxide catalysts. For instance, the traditional supported vanadia on silica catalyst (V/SiO_2) shows 61% of propene selectivity at 9% of propane conversion, with the major byproduct being CO_x at 33% [4]. Also, other types of supported vanadia catalysts such as V/Al_2O_3 and V/TiO_2 are found to exhibit around 63% and 40% of propene selectivity at around 15% of propane conversion, respectively [4, 5]. Revealing the mechanistic picture of unpreceded product distribution and reactivity in boron-containing materials is, therefore, the focus of many recent studies.

Several other groups have investigated hBN catalysts for ODH of light alkanes and confirmed the high olefin selectivity [6–9]. As more boron-containing materials have been investigated, it has been shown that they all exhibit a similar selectivity-conversion ODH trend and only differ in the rate of propane consumption (mol C_3H_8 kg-cat^{-1} s^{-1}) [10]. Detailed spectroscopic characterization (e.g. using Raman, XPS and solid-state NMR) reveals that the ODH activity is correlated with the oxygen functionalization of the hBN catalyst, strongly suggesting its crucial role in the catalytic activity. This hypothesis was confirmed by evaluating the performance of B/SiO_2 and B/carbon materials showing similar catalytic performance and B NMR features as (spent) hBN [11–14]. Beyond the activity, McDermott et al. showed that the selectivity of dehydrogenation versus C–C bond cleavage-the dominant side reaction-is a function of the concentration of oxygen in the gas feed [8, 10]. The reported reaction order of ~2.0 with respect to propane in boron-catalyzed ODH further indicates a mixed surface-gas-phase mechanism [1, 3]. This picture is also aligned with the gas-phase oxidation mechanism proposed in combustion literature [15, 16]. These efforts further led to the hypothesis that ODH over boron-based catalysts proceeds *via* a radical mechanism, and the gas-phase oxidation chemistry is responsible for the unprecedented selectivity of olefin [17–23]. Venegas et al. proposed that the selectivity to olefin is determined by the H-abstracting species to form *n*-propyl radicals (nC_3H_7) and *iso*-propyl radicals (iC_3H_7) (Fig. 1) [17]. The gas-phase activation of propane through $HOO^{\bullet}$ radicals favors the abstraction of secondary H atoms from propane, leading to iC_3H_7/nC_3H_7 ratio of 1.5. In contrast, the surface activation of propane through $>BO^{\bullet}$ radicals favors the abstraction of primary H atoms, leading to iC_3H_7/nC_3H_7 of 0.74. Indeed, *n*-propyl radicals can be converted to ethylene and methyl radicals, and *iso*-propyl radicals yield exclusively propylene [24]. This study points out that the computationally predicted higher reactivity of $>BO^{\bullet}$ radicals, relative to $HOO^{\bullet}$ radicals, makes the surface sites less selective for secondary C-H bonds in propane, in line with common knowledge in free radical chemistry. Building on this network, in a fixed bed configuration, the surface of hBN was found to contribute for about 50% to propane activation with another 50% coming from gas phase chemistry. Therefore, revealing factors to promote the gas-phase propagation is key for the development of more selective boron-containing ODH catalysts.

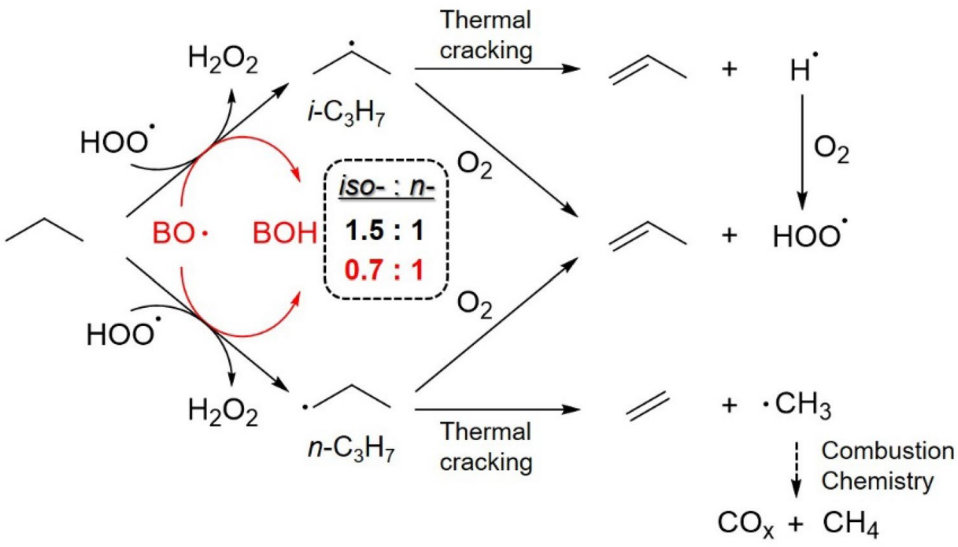

Fig. 1 Simplified reaction network describing the critical steps involved in the mixed surface (red-colored) and gas-phase (black-colored) ODH of propane to propylene and the undesired pathway to ethylene, methane, and carbon oxides; *iso*-:*n*- ratios shown in the Figure illustrate the propyl radical distribution of gas-phase and surface propane H-abstraction [17]

In recent years, the use of 3D printing technology has emerged as an effective method to shape catalysts and adsorbents for various applications [25]. The technique allows for precise control over configuration and composition of the shaped structures while providing the opportunity to fine-tune the surface chemistry before, during, or after printing. In this contribution, we explore the 3D printing methodology to engineer a structured catalyst configuration, with a focus on the impact of propane reaction order and byproduct of ethylene and CO_x during the hBN-catalyzed ODH of propane. The catalytic results of 3D-structured BNK catalysts are compared with those of physical mixture of hBN and kaolinite pellets. Also, the long-term durability of 3D-printed catalysts was examined as a function of time for two weeks. The physicochemical properties of 3D-printed catalysts prepared here have been characterized using environmental scanning electron microscope (ESEM) and Fourier-transform infrared (FT-IR) spectroscopy.

2 Experimental

2.1 3D-Printed hBN Monoliths

Hexagonal boron nitride (hBN, 99.5%) was purchased from Alfa Aesar, while kaolinite and methylcellulose (MC, 99%) were obtained from Sigma-Aldrich. In a typical synthesis, 1.0 g of BN powders was oxyfunctionalized in a quartz reactor tube (12 mm O.D. × 8 mm I.D. × 36 cm) under ODHP conditions ($T = 525$ °C, $P = 0.3$ atm C_3H_8, 0.15 atm O_2, 0.55 atm N_2) for 12 h. Desired amounts of oxyfunctionalized BN, kaolinite, and methylcellulose were mixed with DI water and well mixed to a slurry over 48 h. The slurry is then stirred vigorously and heated gently until a paste is formed. Rheological tests of the paste were done to determine a synthetic protocol that produced "ink" suitable for 3D printing, and the ink was transferred into a syringe barrel with a 1.65 cm diameter (Nordson, EFD), fitted to a cylindrical nozzle of 0.84 mm diameter (Nordson, EFD). Monoliths were 3D-printed to the cylinder structure of 7 mm length and 10 mm with a body center tetrahedral symmetry and a rod spacing of 2 mm. The 3D-printed hBN catalysts were dried at room temperature. A more-detailed description of the paste formation and printing of the structured monoliths can be found in our recent papers [26–28]. The amount of oxyfunctionalized hBN catalysts was adjusted, relative to the amount of kaolinite and denoted as X_BNK (X represents the weight% of hBN catalysts in the mixture). Two different weight percentages of hBN catalysts in resulting 3D-printed monoliths were investigated, including 5_BNK and 50_BNK. The 3D-printed sample without hBN catalysts were prepared as a control and denoted as 0_BNK. N_2 physisorption measurements indicated that the fresh monoliths (i.e., 0, 5, and 50_BNK) had BET surface areas of 15, 16, and 25 m^2/g, while the fresh pellets (i.e., hBN, kaolinite, and BN- kaolinite) had BET surface areas of 7, 11, and 9 m^2/g, respectively.

2.2 Catalytic Reaction Studies

Catalytic reactions were carried out in a Microactivity Effi Microreactor (PID Eng. & Tech) equipped with 3 EL Flow Bronkhorst Mass Flow controllers which individually controlled the delivery of N_2, O_2, and C_3H_8 to the catalyst bed. Catalyst pellets in 425–625 µm and monoliths were loaded into a quartz reactor tube (12 mm O.D. × 8 mm I.D. × 36 cm) packed with quartz chips such that the catalyst bed was centered between two quartz wool plugs. In each test, ~ 80 and 400 mg of catalyst pellets and monoliths were diluted with 500 mg of quartz chips (0.5–1 mm quartz chips, Pyromatics) to obtain a catalyst bed height of ~ 0.8 inches, respectively. A thermocouple (k-type) sat in the center of the catalyst bed. The reactor tube was placed into a split tube furnace within a hot box heated to 160 °C for all experiments. Reactive gas mixture was fed top-down through the reactor tube. In a typical ODH run, the furnace was heated to 550 °C under 30 mL_n min^{-1} N_2 and 10 mL_n min^{-1} O_2 and held under these conditions for at least 1 h after the temperature stabilized. The catalyst was then heated to the desired temperature for reaction testing. Typically, the gas mixture was held at 30% C_3H_8, 15% O_2, and 55% N_2 and the total flow rate was changed between 20 and 120 mL min^{-1}, unless otherwise stated. Sample was treated under these conditions until steady state was achieved. Less than 1% conversion was observed under these conditions at 500 °C in a blank quartz reactor tube packed with quartz chips. Once contacted with the catalyst bed, the reaction effluent was fed to a thermoelectrically cooled condensing unit maintained at − 2 °C, which was emptied periodically to avoid accumulation of condensed liquid. Dried effluent was then analyzed *via* online gas chromatography (GC Shimadzu 2010) fit with parallel lines: Hayesep QBond, RT-QBond, and Mol Sieve 5 A lines to a TCD and RTX-1 (or GS-Gaspro) lines to an FID. He (UHP) was used as the carrier gas. N_2 was used as an internal standard for all experiments and an average of 5 GC measurements were taken per data point (e.g., conversion, selectivity, reaction rate, etc.) with an average standard deviation < 1%. All carbon balance closed within 3% for all experiments.

The reaction orders were obtained from the slope of the reaction rate of propane (r_{C3H8}), which was calculated as follows:

$$rC_3H_8 = F_{C_3H_8} \times X_{C_3H_8}/M_{cat.}$$

where F_{C3H8}, X_{C3H8}, and M_{cat} are the molar flow rate of C_3H_8 at the inlet of the reactor, the conversion of C_3H_8, and the weight of the catalyst, respectively.

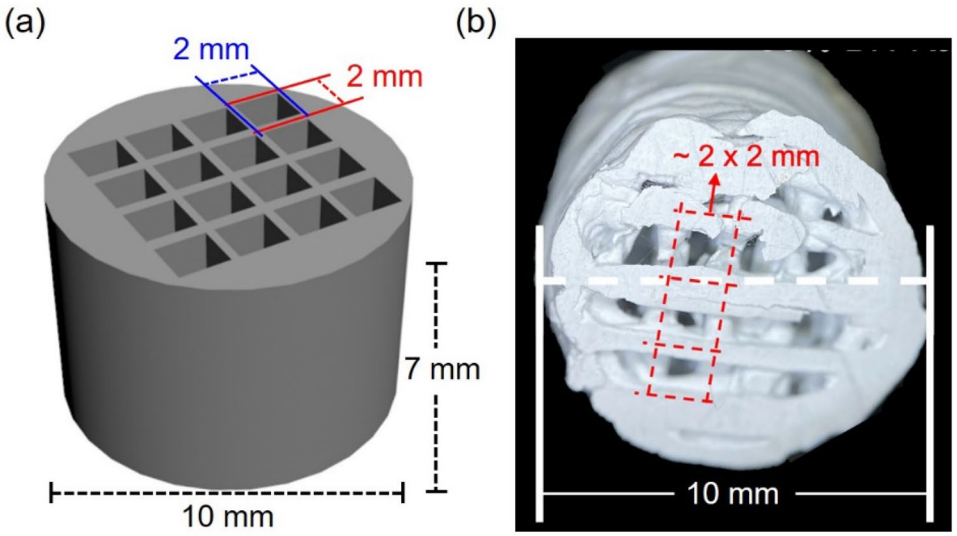

Fig. 2 **a** Schematic illustration of 3D-printed hBN monoliths with relevant dimensions. **b** SEM image of 3D-printed hBN monoliths using kaolinite as the binder

2.3 ESEM and ATR Characterizations

The geometric properties of 3D-printed hBN monoliths was measured by using a Quanta 600 F environmental scanning electron microscope (ESEM) at RT. The Fourier-transform infrared (FT-IR) spectra were collected using a Bruker 70 MID-IR Spectrometer with a MIRacle™ Single Reflection ATR from PIKE Technologies for Attenuated total reflectance (ATR) analysis. The IR measurements were carried out by introducing the samples on the ATR crystal.

3 Results and Discussion

It is worth mentioning that the oxygen functionalization of hBN during ODH reaction is critical to ODH reactivity. Before fabricating 3D-printed samples with hBN, therefore, the hBN catalysts were oxyfunctionalized under ODHP conditions ($T = 525$ °C, $P = 0.3$ atm C_3H_8, 0.15 atm O_2, 0.55 atm N_2) for 12 h and used freshly to prepare a catalyst slurry with binder material for 3D printing. Details can be found in the 2 Section. The dimensions of a typical 3D-printed sample are shown in Fig. 2. The 3D-printed monolith has a cylindrical structure measuring 7 mm in length and 10 mm in width, featuring a tetrahedral symmetry at the body center and a rod spacing of 2 mm (Fig. 2a). In addition, 3D-printed hBN catalysts using the monolith was uniformly fabricated through 3D printing technique. The resulting material shows a structure with orthogonally interconnected rods (Fig. 2b).

Next, we investigated the difference in reactivity of 3D-printed hBN catalysts. Experimental details can be found in the 2 Section. ODH of propane to propylene was examined at a reaction temperature of 525 °C using a reaction gas consisting of 0.3 atm C_3H_8, 0.15 atm O_2, 0.55 atm N_2. The blank experiment with the quartz reaction tube loaded with kaolinite show propane conversion of less than 1.0%, suggesting kaolinite is not active for ODH of propane. Figure 3 summarizes the selectivity of 3D-printed catalysts and compares them to two control samples under packed bed configurations, including hBN catalysts and the physical mixture of hBN catalysts and kaolinite. The selectivity profiles between these samples were compared at a similar conversion of propane (~4%). The sample of hBN catalysts under packed bed configurations, serving as a control, showed a propylene selectivity at around 83.5% in agreement with the literature. Another control experiment of the 3D-printed sample without hBN catalysts (0_BNK) exhibited higher reactivity than a packed bed of kaolinite but produced large amounts of CO_x (48.5%). After introducing hBN into the 3D-printed monolith, the selectivity to CO_x reduced to nearly undetectable levels in 50_BNK with a propylene selectivity of 90.5%. To investigate the enhanced selectivity to propylene, we examined the physical mixture of hBN catalysts and kaolinite (Packed bed BN-kaolinite). The physical mixture showed enhanced selectivity to propylene but with observable amounts of CO_x. The nearly negligible formation of CO_x in the 3D-printed hBN catalysts suggests that structuring catalysts through 3D printing technique indeed influences the ODH of propane.

Having observed the enhanced ODH performance in 3D-printed hBN catalysts, we aimed to better understand its physicochemical basis. As such, we experimentally investigated the rates of propylene and ethylene formation ($r_{propylene}/r_{ethylene}$) as a function of oxygen concentration from 2.5 to 25%, and the results are presented in Fig. 4. Rates of propylene and ethylene formation could gauge the selectivity of dehydrogenation versus C–C bond cleavage. As shown in Fig. 4, 3D-printed catalysts of 50_BNK exhibited much higher $r_{propylene}/r_{ethylene}$ values compared to the controlled catalyst (physical mixture under packed bed configurations),

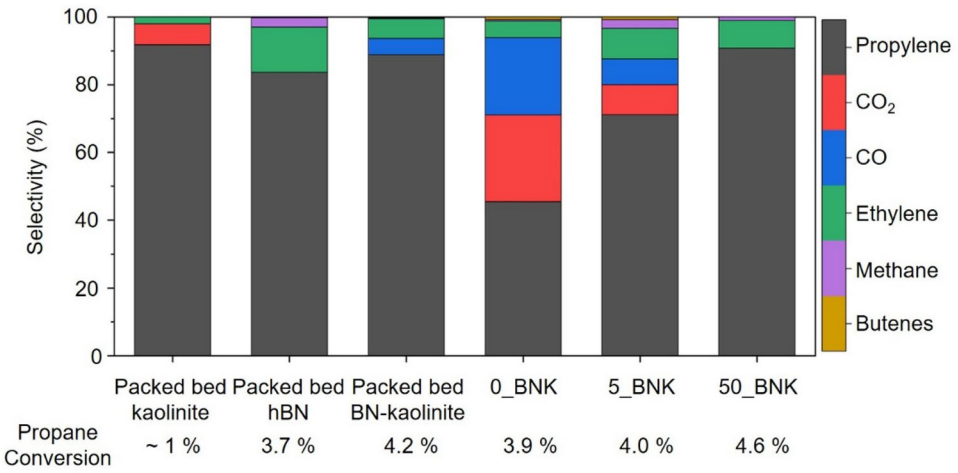

Fig. 3 Isoconversion comparison of kaolinite, hBN, the physical mixture of hBN and kaolinite, and structured catalysts. Reaction condition: $T = 525$ °C, $P = 0.3$ atm C_3H_8, 0.15 atm O_2, 0.55 atm N_2

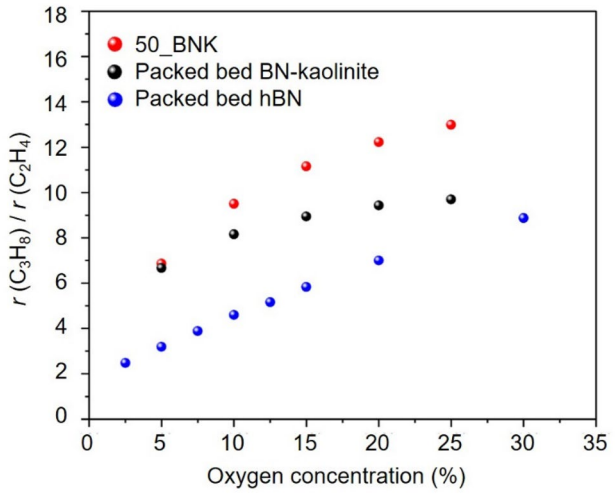

Fig. 4 Rates of propylene and ethylene formation as a function of oxygen concentration for hBN, the physical mixture of hBN and kaolinite, and 50_BNK. Reaction condition: $T = 525$ °C, $P = 0.3$ atm C_3H_8 with N_2 as the balancing gas to maintain the total pressure of 1.0 atm

suggesting that the change in reactor configuration contributed to the promotion of C–H activation over C–C cracking.

To further investigate the promoted C–H scission over C–C cracking, we examined the reaction order of propane and oxygen in 3D-printed catalysts of 50_BNK. The physical mixture of hBN catalysts and kaolinite under packed-bed configurations was again evaluated as control experiment. The rate of propane consumption (mol C_3H_8 kg-cat^{-1} s^{-1}) was examined as a function of oxygen and propane, respectively. As shown in Fig. 5, the physical mixture showed a reaction order of propane and oxygen at 1.45 and 0.25, respectively. In contrast, the 3D-printed catalysts of 50_BNK exhibited a much higher propane reaction order of 2.27, which is higher than the reported reaction order of ~2.0 with respect to propane in the boron-catalyzed ODH of propane [4]. The higher propane reaction order in 3D-printed catalysts of 50_BNK combined with the promotion of C–H scission over C–C cracking implied the promotion of gas-phase reaction.

Next, we examined the stability of the 3D-printed catalysts of 50_BNK. As shown in Fig. 6, we demonstrate that 15.8% propane conversion with propylene and ethylene selectivities of 78.4% and 11.6%, respectively, can be steadily maintained for two weeks over 3D-printed catalysts of 50_BNK. This two-week stability assessment surpasses the previous investigation on hBN catalysts (i.e., 15 to 100 h) [10, 29], and suggests that the hBN-catalyzed ODH of propane is indeed stable even after more than 300 h of time-on-stream. By increasing the contact time for an additional 42 h, we also show that 3D-printed catalysts of 50_BNK can exhibit a higher performance at 32% propane conversion with propylene and ethylene selectivities of 63.6% and 15.7%, respectively. At this condition, we achieve ~20% propylene yield and ~25% total olefin yield.

To better understand the property-performance relations in the 3D-printed hBN catalysts, we carried out Attenuated Total Reflectance IR (ATR-IR) measurements to characterize the material before (demoted as fresh) and after (denoted as spent) exposure to the ODH of propane. Pure kaolinite powders were compared with the fresh and spent 50_BNK samples and the difference in the spectral region between 3800 cm^{-1} and 3000 cm^{-1} associated with –OH stretching, likely C–C cracking sites [30], was monitored. As illustrated in Fig. 7, both fresh kaolinite and fresh 50_BNK exhibit a series of similar spectral signatures from 3700 cm^{-1} to 3600 cm^{-1}, which were attributed to the –OH stretching of hydroxyl groups in kaolinite [31]. The additional signature observed at 3215 cm^{-1} in fresh 50_BNK is attributed to B–OH groups [32], which may serve as surface sites to facilitate the ODH reaction. Notably, all bands between

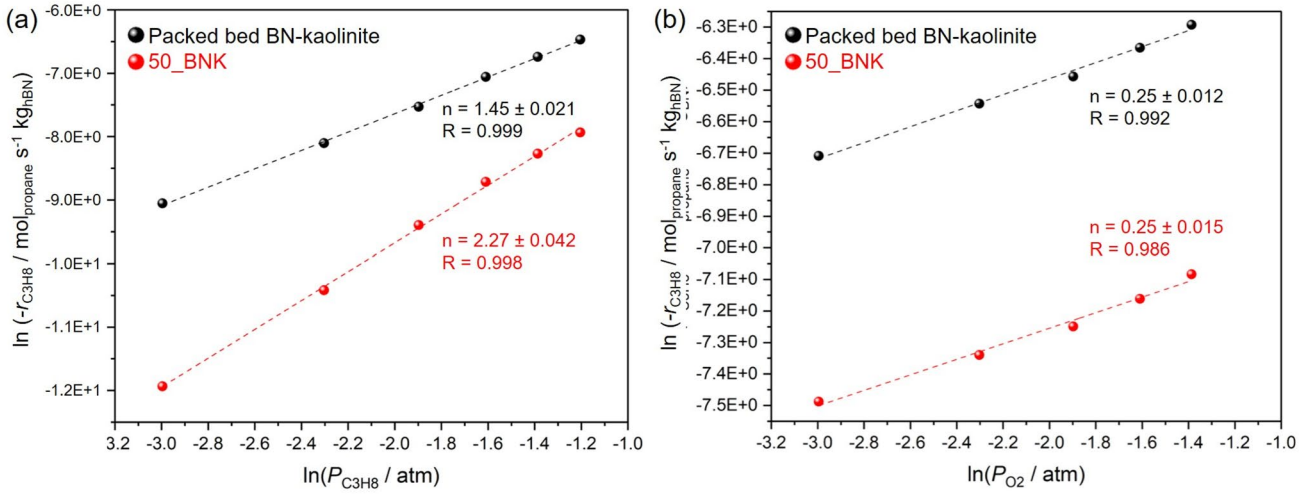

Fig. 5 Dependence of the propane consumption rate on (**a**) propane partial pressure at $P_{O2} = 0.15$ atm and (**b**) oxygen partial pressure at $P_{C3H8} = 0.30$ atm. $T = 525$ °C, $P_{tot} = 1$ atm with N_2 as the balance gas

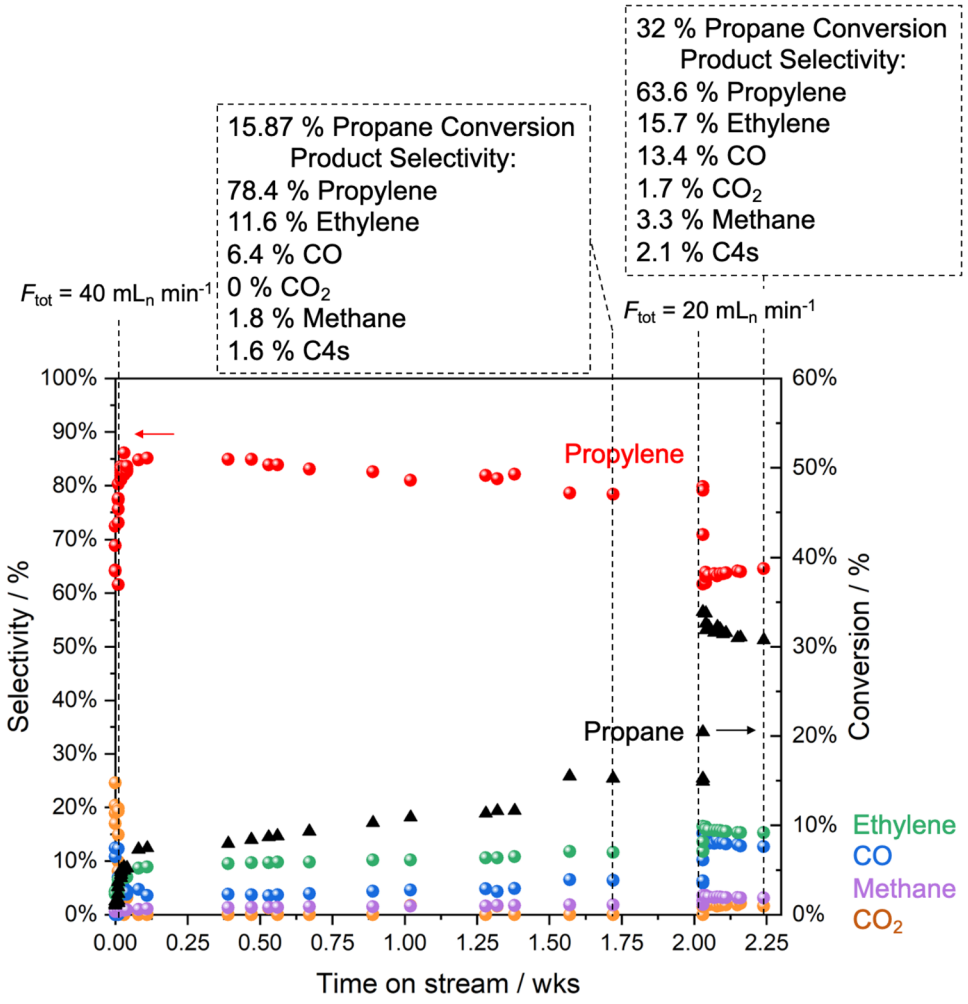

Fig. 6 Assessment of catalyst stability with 3D-printed catalysts of 50_BNK as a function of time on stream. $T = 525$ °C, $P = 0.3$ atm C_3H_8, 0.15 atm O_2, 0.55 atm N_2

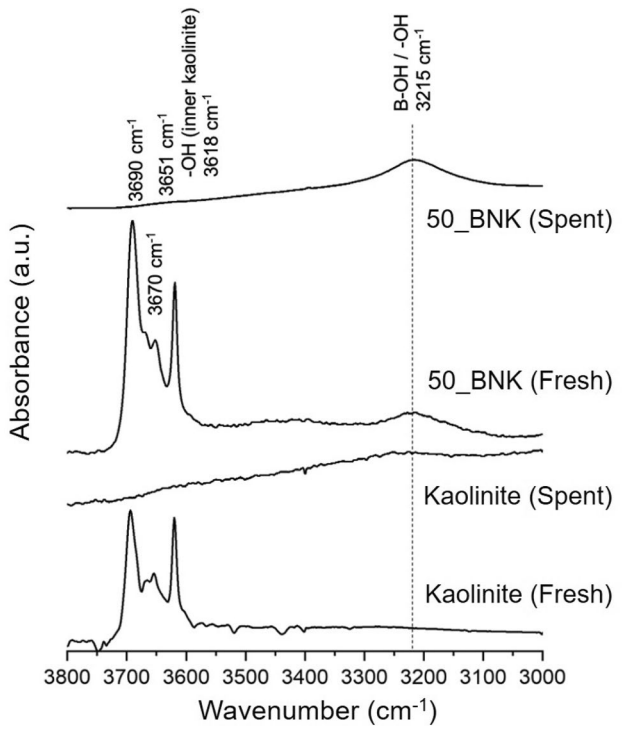

Fig. 7 ATR-IR spectra of fresh and spent kaolinite powders and fresh and spent 50_BNK monoliths. All spectra were recorded at room temperature under atmospheric conditions

3700 cm^{-1} and 3600 cm^{-1} are no longer observed in spent kaolinite or 50_BNK, suggesting that the hydroxyl groups in kaolinite were eliminated upon dehydration. In contrast, the signature of B–OH groups observed at 3215 cm^{-1} remains intense in spent 50_BNK. Collectively, these results indicate that the surface of 50_BNK is dominated by B–OH groups with minimal amounts of hydroxy groups from kaolinite, implying that B–OH groups may play key roles in ODH reaction.

4 Conclusions

In this work, we explored the applicability of 3D printing technique to engineer a structured catalyst configuration and examined its impact on the observed ODH reactivity of propane. Our experimental results showed the promoted propylene selectivity with nearly no CO_x formation when the structured catalyst was used. Control experiments examining the physical mixture of hBN and kaolinite indicated that the promoted performance could not be explained by the increased homogeneity of hBN throughout the catalyst bed. The promoted ODH performance of 3D-printed hBN catalyst may be rooted in the enhanced contribution of gas-phase reaction, as evidenced by the increase of propane reaction order from 1.5 to 2.3. The higher reaction order of propane observed in 3D-printed hBN monoliths, coupled with a reduced formation of byproducts, is consistent with the increased role of gas-phase reactions. Infrared spectroscopic observations suggested that the B-OH groups may play key roles in ODH reaction. This work serves as a step forward to confirm the state-of-the-art reaction mechanism and illustrates the power of molecular level insights in selective oxidation chemistry to improve the performance.

Acknowledgements The authors acknowledge financial support of the U.S. Department of Energy. Office of Science, Office of Basic Energy Science, under award DE-SC0017918 (catalytic and mechanistic investigation of boron-based ODH catalysts) and the National Science Foundation Graduate Research Fellowship Program under Grant No. DGE-1747503. The authors also acknowledge financial support from National Science Foundation under Grant No. IIP-2044726 (3D printing of catalysts).

Declarations

Competing interests The authors declare they have no financial interests.

References

1. Venegas JM, McDermott WP, Hermans I (2018) Serendipity in catalysis research: boron-based materials for alkane oxidative dehydrogenation. Acc Chem Res 51(10):2556–2564. https://doi.org/10.1021/acs.accounts.8b00330
2. Tian J, Lin J, Xu M, Wan S, Lin J, Wang Y (2018) Hexagonal boron nitride catalyst in a fixed-bed reactor for exothermic propane oxidation dehydrogenation. Chem Eng Sci 186:142–151. https://doi.org/10.1016/j.ces.2018.04.029
3. Shi L, Wang Y, Yan B, Song W, Shao D, Lu A-H (2018) Progress in selective oxidative dehydrogenation of light alkanes to olefins promoted by boron nitride catalysts. Chem Commun 54(78):10936–10946. https://doi.org/10.1039/C8CC04604B
4. Grant JT, Carrero CA, Goeltl F, Venegas J, Mueller P, Burt SP, Specht SE, McDermott WP, Chieregato A, Hermans I (2016) Selective oxidative dehydrogenation of propane to propene using boron nitride catalysts. Science 354(6319):1570–1573. https://doi.org/10.1126/science.aaf7885
5. Cavani F, Ballarini N, Cericola A (2007) Oxidative dehydrogenation of ethane and propane: how far from commercial implementation? Catal Today 127(1–4):113–131. https://doi.org/10.1016/j.cattod.2007.05.009
6. Lu W-D, Wang D, Zhao Z, Song W, Li W-C, Lu A-H (2019) Supported boron oxide catalysts for selective and low-temperature oxidative dehydrogenation of propane. ACS Catal 9(9):8263–8270. https://doi.org/10.1021/acscatal.9b02284
7. Shi L, Wang D, Song W, Shao D, Zhang W-P, Lu A-H (2017) Edge-hydroxylated boron nitride for oxidative dehydrogenation of propane to propylene. ChemCatChem 9(10):1788–1793. https://doi.org/10.1002/cctc.201700004
8. Venegas JM, Grant JT, McDermott WP, Burt SP, Micka J, Carrero CA, Hermans I (2017) Selective oxidation of n-Butane and isobutane catalyzed by boron nitride. ChemCatChem 9(12):2118–2127. https://doi.org/10.1002/cctc.201601686
9. Yan B, Li W-C, Lu A-H (2019) Metal-free silicon boride catalyst for oxidative dehydrogenation of light alkanes to olefins with high

selectivity and stability. J Catal 369:296–301. https://doi.org/10.1016/j.jcat.2018.11.014
10. McDermott WP, Venegas J, Hermans I (2020) Selective oxidative cracking of n-Butane to light olefins over Hexagonal Boron Nitride with limited formation of CO_x. Chemsuschem 13(1):152–158. https://doi.org/10.1002/cssc.201901663
11. Love AM, Thomas B, Specht SE, Hanrahan MP, Venegas JM, Burt SP, Grant JT, Cendejas MC, McDermott WP, Rossini AJ, Hermans I (2019) Probing the transformation of boron nitride catalysts under oxidative dehydrogenation conditions. J Am Chem Soc 141(1):182–190. https://doi.org/10.1021/jacs.8b08165
12. Love AM, Cendejas MC, Thomas B, McDermott WP, Uchupalanun P, Kruszynski C, Burt SP, Agbi T, Rossini AJ, Hermans I (2019) Synthesis and characterization of silica-supported boron oxide catalysts for the oxidative dehydrogenation of propane. J Phys Chem C 123(44):27000–27011. https://doi.org/10.1021/acs.jpcc.9b07429
13. Cendejas MC, Dorn RW, McDermott WP, Lebron-Rodriguez EA, Mark LO, Rossini AJ, Hermans I (2021) Controlled grafting synthesis of silica-supported boron for oxidative dehydrogenation catalysis. J Phys Chem C 125(23):12636–12649. https://doi.org/10.1021/acs.jpcc.1c01899
14. Mark LO, Dorn RW, McDermott WP, Agbi TO, Altvater NR, Jansen J, Lebrón-Rodríguez EA, Cendejas MC, Rossini AJ, Hermans I (2021) Highly selective carbon-supported boron for oxidative dehydrogenation of propane. ChemCatChem 13(16):3611–3618. https://doi.org/10.1002/cctc.202100759
15. Hashemi H, Christensen JM, Harding LB, Klippenstein SJ, Glarborg P (2019) High-pressure oxidation of propane. Proc Combust Inst 37(1):461–468. https://doi.org/10.1016/j.proci.2018.07.009
16. Warnatz J (1984) Rate coefficients in the C/H/O system. In: Gardiner WC (ed) Combustion Chemistry. Springer, New York, pp 197–360. https://doi.org/10.1007/978-1-4684-0186-8_5
17. Venegas JM, Zhang Z, Agbi TO, McDermott WP, Alexandrova A, Hermans I (2020) Why boron nitride is such a selective catalyst for the oxidative dehydrogenation of propane. Angew Chem Int Ed 59(38):16527–16535. https://doi.org/10.1002/anie.202003695
18. Kraus P, Lindstedt RP (2021) It's a gas: oxidative dehydrogenation of propane over boron nitride catalysts. J Phys Chem C 125(10):5623–5634. https://doi.org/10.1021/acs.jpcc.1c00165
19. Venegas JM, Hermans I (2018) The influence of reactor parameters on the boron nitride-catalyzed oxidative dehydrogenation of propane. Org Process Res Dev 22(12):1644–1652. https://doi.org/10.1021/acs.oprd.8b00301
20. Liu Y, Liu Z, Wang D, Lu A-H (2022) Suppressing deep oxidation by detached nano-sized boron oxide in oxidative dehydrogenation of propane revealed by the density functional theory study. J Phys Chem C 126(50):21263–21271. https://doi.org/10.1021/acs.jpcc.2c06910
21. Liu Z, Lu W-D, Wang D, Lu A-H (2021) Interplay of on- and off-surface processes in the B_2O_3-catalyzed oxidative dehydrogenation of propane: a DFT study. J Phys Chem C 125(45):24930–24944. https://doi.org/10.1021/acs.jpcc.1c07690
22. Tian J, Tan J, Xu M, Zhang Z, Wan S, Wang S, Lin J, Wang Y (2019) Propane oxidative dehydrogenation over highly selective hexagonal boron nitride catalysts: the role of oxidative coupling of methyl. Sci Adv 5(3):eaav8063. https://doi.org/10.1126/sciadv.aav8063
23. Zhang X, You R, Wei Z, Jiang X, Yang J, Pan Y, Wu P, Jia Q, Bao Z, Bai L, Jin M, Sumpter B, Fung V, Huang W, Wu Z (2020) Radical chemistry and reaction mechanisms of propane oxidative dehydrogenation over hexagonal boron nitride catalysts. Angew Chem Int Ed 59(21):8042–8046. https://doi.org/10.1002/anie.202002440
24. Curran HJ (2006) Rate constant estimation for C1 to C4 alkyl and alkoxyl radical decomposition. Int J Chem Kinet 38(4):250–275. https://doi.org/10.1002/kin.20153
25. Lawson S, Li X, Thakkar H, Rownaghi AA, Rezaei F (2021) Recent advances in 3D printing of structured materials for adsorption and catalysis applications. Chem Rev 121(10):6246–6291. https://doi.org/10.1021/acs.chemrev.1c00060
26. Lawson S, Baamran K, Newport K, Garcia E, Jacobs G, Rezaei F, Rownaghi AA (2022) Adsorption-enhanced bifunctional catalysts for in situ CO_2 capture and utilization in propylene production: a proof-of-concept study. ACS Catal 12(22):14264–14279. https://doi.org/10.1021/acscatal.2c04455
27. Lawson S, Baamran K, Newport K, Alghamadi T, Jacobs G, Rezaei F, Rownaghi AA (2022) Integrated direct air capture and oxidative dehydrogenation of propane with CO_2 at isothermal conditions. Appl Catal B 303:120907. https://doi.org/10.1016/j.apcatb.2021.120907
28. Baamran K, Rownaghi AA, Rezaei F (2023) Direct synthesis of ethylene and hydrogen from CO_2 and ethane over a bifunctional structured CaO/Cr_2O_3-V_2O_5/ZSM-5 adsorbent/catalyst monolith. ACS Sustain Chem Eng 11(3):1006–1018. https://doi.org/10.1021/acssuschemeng.2c05627
29. Wang Y, Li W-C, Zhou Y-X, Lu R, Lu A-H (2020) Boron nitride wash-coated cordierite monolithic catalyst showing high selectivity and productivity for oxidative dehydrogenation of propane. Catal Today 339:62–66. https://doi.org/10.1016/j.cattod.2018.12.028
30. Rong T-J, Xiao J-k (2002) The catalytic cracking activity of the kaolin-group minerals. Mater Lett 57(2):297–301. https://doi.org/10.1016/S0167-577X(02)00781-4
31. Prost R, Dameme A, Huard E, Driard J, Leydecker JP (1989) Infrared study of structural OH in kaolinite, dickite, nacrite, and poorly crystalline kaolinite at 5 to 600 K. Clays Clay Miner 37(5):464–468. https://doi.org/10.1346/CCMN.1989.0370511
32. Nautiyal P, Loganathan A, Agrawal R, Boesl B, Wang C, Agarwal A (2016) Oxidative unzipping and transformation of high aspect ratio boron nitride nanotubes into "white graphene oxide" platelets. Sci Rep 6(1):29498. https://doi.org/10.1038/srep29498

Authors and Affiliations

Theodore Agbi[1] · Wei-Shang Lo[2] · Khaled Baamran[4] · Taekyung Ryu[2] · Christine Cheung[2] · Fateme Rezaei[4] · Ive Hermans[1,2,3]

[1] Department of Chemical and Biological Engineering, University of Wisconsin–Madison, 1415 Engineering Drive, Madison, WI 53706, USA

[2] Department of Chemistry, University of Wisconsin–Madison, 1101 University Avenue, Madison, WI 53706, USA

[3] Wisconsin Energy Institute, University of Wisconsin–Madison, 1552 University Avenue, Madison, WI 53726, USA

[4] Department of Chemical & Biochemical Engineering, Missouri University of Science and Technology, 1101 N State Street, Rolla, MO 65409, USA